



**HAL**  
open science

# Differential Passive Circuit Modelling with Pentapole Impedance Matrices Application to an Integrated Audio Switching Amplifier for Portable Devices

Roberto Mrad, Florent Morel, Gaël Pillonnet, Christian Vollaire, Denis Labrousse

## ► To cite this version:

Roberto Mrad, Florent Morel, Gaël Pillonnet, Christian Vollaire, Denis Labrousse. Differential Passive Circuit Modelling with Pentapole Impedance Matrices Application to an Integrated Audio Switching Amplifier for Portable Devices. EMC, 2011, York, United Kingdom. hal-01103635

**HAL Id: hal-01103635**

**<https://hal.science/hal-01103635>**

Submitted on 15 Jan 2015

**HAL** is a multi-disciplinary open access archive for the deposit and dissemination of scientific research documents, whether they are published or not. The documents may come from teaching and research institutions in France or abroad, or from public or private research centers.

L'archive ouverte pluridisciplinaire **HAL**, est destinée au dépôt et à la diffusion de documents scientifiques de niveau recherche, publiés ou non, émanant des établissements d'enseignement et de recherche français ou étrangers, des laboratoires publics ou privés.

# Differential Passive Circuit Modelling with Pentapole Impedance Matrices

## Application to an Integrated Audio Switching Amplifier for Portable Devices

Roberto Mrad<sup>1,2</sup>, Florent Morel<sup>2</sup>, Gael Pillonnet<sup>1</sup>, Christian Vollaire<sup>2</sup>, Denis Labrousse<sup>2</sup>

<sup>1</sup>University of Lyon, CPE

INL, UMR CNRS 5270

43, bd de 11 Novembre 1918

69616 Villeurbanne cedex – France

firstname.lastname@cpe.fr

<sup>2</sup>University of Lyon, Ecole Centrale de Lyon

Ampère, UMR CNRS 5005

36, avenue Guy de Collongue

69134 ECULLY cedex – France

firstname.lastname@ec-lyon.fr

**Abstract**— In this paper a novel method to model the passive parts of differential output system is presented. This approach, based on impedance matrices, models conducted EMI and takes into account component non-idealities. It is not only able to deal with common mode but also differential mode and with conversion between the two modes. This method is experimentally applied to the passive output part of an audio differential switching amplifier dedicated to mobile phone applications. Using a simple impedance-meter, results show good accuracy up to 110 MHz when associating the different parts of the system.

**Keywords**- conducted EMI; frequency domain modeling; impedance matrices; passive circuit modeling

### I. INTRODUCTION

Speed, size and energy efficiency are the biggest challenges for embedded systems manufacturers at the moment. Embedded systems are based on extremely small integrated circuits, where thinner the submicron technology, the more sensitive it is to EMI (Electro Magnetic Interference) perturbations. Moreover, the use of high potential aggressor circuits (such as the switching power management circuits), introduces some practical EMI problems during the final development stage of portable devices. Thus, the intra-circuit EMC (Electro Magnetic Compatibility) can no longer be neglected by manufacturers. For this purpose, the conducted EMIs and even the radiated EMIs [1-2] in portable devices are widely studied today, and should be represented accurately in today's simulations in order to avoid prototypes that cost time and money.

In the case of integrated audio applications in mobile phones, the switching converter topologies (Fig.1) are widely

used due to the high power efficiency. A typical Class D topology is composed of H-bridge switching power stages integrated in submicronic CMOS technology. The switching frequency is between 300 kHz and 2 MHz, the rise and fall times of output voltages are less than 10ns, switching up to 1A. The switching nature of the audio amplifier generates undesired high frequencies, and disturbs surrounding electronics such as digital ICs and RF components. Therefore, to reduce the unwanted EM interactions, a costly and large passive output filter is introduced. Furthermore, other complex circuits [3-4] and techniques are explored in order to improve the EMIs, like the spread spectrum [5-8].

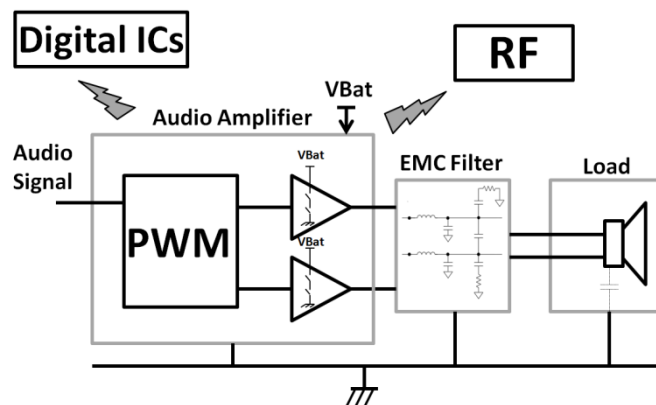


Figure 1. Class D amplifier block decomposition

In order to solve the undesired EMI problems, it is necessary to start by finding a suitable way to model the EMI frequency behavior of the switching audio amplifier, without using time domain simulations, because of their huge

simulation time and their inaccuracy at high frequencies. As passive elements have a significant impact on conducted EMIs, and the amplifier chip is an already designed black box (its emission can be measured using a specific testing board [9]), the passive parts of the system (filter, load and tracks etc) are the EMI reduction tools. Therefore a tool that can model these parts at the design stage for a normative comparison would be useful. Dividing the system into blocks allows the designers to isolate the defects for better treatment and predict the impact on the whole system by changing only a single block. Previous work used this approach for common mode modeling using 2x2 impedance matrices to represent each block of the system [9-11]. However, in the case of differential systems (like differential class D audio amplifier) this model cannot be used if differential mode and mode conversion have to be taken into account. Other models, as those in [12-13], deal with differential mode, common mode and mode conversion for a single passive block without studying a whole system. Another way used to model passive networks consists in extracting parasitic elements of conductors (PCB, busbar and cables etc) and to characterize separately each discrete component. Several softwares using different numerical methods [14-15] allow stray elements of the implemented geometry to be extracted. This kind of method is only efficient for simple geometries. Intrinsic stray elements of discrete components can be provided by manufacturers or extracted from the measurements.

This paper presents a pentapolar model able to represent the passive output parts of a system with two active conductors and a grounded conductor. This model allows conducted EMI to be calculated directly in the frequency domain that leads to a shorter simulation time. Moreover, differential and common mode disturbances as well as mode conversion are taken into account, with the intention of using this model at the early design stage.

The next section describes the pentapolar approach. In section III, the proposed approach is experimentally validated on a passive filter and a speaker load for class D amplifier. Section IV concludes.

## II. PENTAPOLAR APPROACH

The Pentapolar approach consists in decomposing the system which includes three conductors (2 active conductors and a ground reference), into sub-systems as shown in Fig.1. Each passive sub-system is represented by a pentapolar block. Blocks are then cascaded to rebuild the system in a black box behavioral model. The associated blocks can be used to calculate the information needed on the output (differential or common modes) for any type of input (differential or common input etc).

### A. Pentapolar block representation

A pentapole can be thought of as a black box with two voltages and two currents on its input as well as on its output. Each pentapolar passive block can be mathematically represented with a 4x4 impedance matrix as shown in Fig.2.

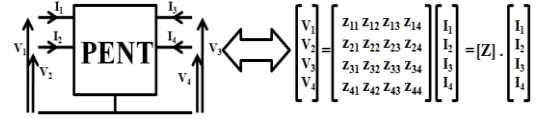


Figure 2. Pentapole mathematical representation

### B. Single matrix parameter evaluation

Determining the matrix elements is divided in two parts. The first is to determine the diagonal elements ( $z_{ii}$  with  $i = 1...4$ ) and the second is to determine the cross elements of the matrix ( $z_{ij}$  with  $j \neq i$ ;  $i=1...4$ ;  $j=1...4$ ). It must be noted that the impedance matrix is symmetric with respect to the diagonal, according to the reciprocity theorem. In fact,  $z_{ii}$  is the impedance seen from the  $i$  port when  $I_j = 0$  ( $j \neq i$ ;  $j=1, \dots, 4$ ).  $z_{ii}$  can be determined using one of three different methods:

- Direct measurement (example shown in Fig.3.a)
- Calculation from the measured impedance of the circuit elements (resistor, inductor and capacitor etc), in order to determine the matrix without a prototype
- Using analytical methods (PEEC, MoM or FEM etc), for track modeling for example

The  $z_{ij}$  terms can be measured directly using the transfer function between the inserted current on the  $j$  port and the measured voltage on the  $i$  port. Otherwise, it can be obtained from (2) that is induced from (1), for a calculation using a simple impedance meter.  $z_{ijsc}$  is the impedance seen from  $i$  port with  $V_j=0$  ( $j \neq i$ ;  $j=1, \dots, 4$ ), and can be obtained in the same way as  $z_{ii}$  (see Fig.3.b).

$$\begin{cases} V_i = z_{i1} \times I_1 + z_{i2} \times I_2 + z_{i3} \times I_3 + z_{i4} \times I_4 \\ V_j = z_{j1} \times I_1 + z_{j2} \times I_2 + z_{j3} \times I_3 + z_{j4} \times I_4 \\ V_j = 0; I_n = 0; i \neq j; n \neq i; n \neq j \end{cases} \quad (1)$$

$$z_{ij} = \sqrt{z_{jj}(z_{ii} - z_{ijsc})} \quad (2)$$

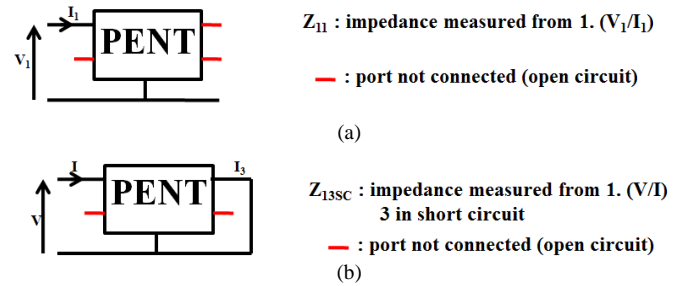


Figure 3.  $z_{ii}$  and  $z_{ijsc}$  determination technique

### C. Block association

The association of the different blocks allows the system to be rebuilt in a single block that models the behavior of all the blocks in a simple matrix. Pentapolar blocks can be cascaded by using the transfer matrix as shown in Fig.4. The

transformation from impedance matrix (Z) to transfer matrix (T) and vice versa can be done using (4) and (5), respectively.

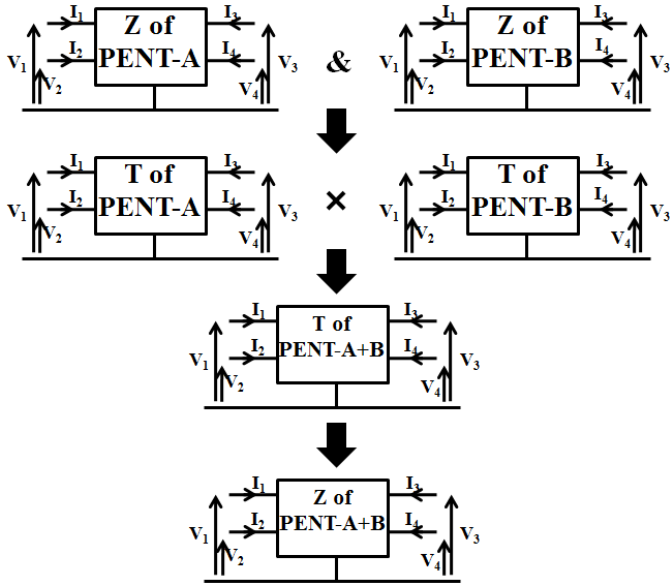


Figure 4. Pentapole association technique

$$\begin{bmatrix} V_3 \\ V_4 \\ I_3 \\ I_4 \end{bmatrix} = \begin{bmatrix} t_{11} & t_{12} & t_{13} & t_{14} \\ t_{21} & t_{22} & t_{23} & t_{24} \\ t_{31} & t_{32} & t_{33} & t_{34} \\ t_{41} & t_{42} & t_{43} & t_{44} \end{bmatrix} \cdot \begin{bmatrix} V_1 \\ V_2 \\ -I_1 \\ -I_2 \end{bmatrix} = [T] \cdot \begin{bmatrix} V_1 \\ V_2 \\ I_1 \\ I_2 \end{bmatrix}$$

Since the T matrix gives the outputs ( $V_3, V_4, I_3, I_4$ ) in terms of the inputs ( $V_1, V_2, I_1, I_2$ ), (3) can be used to calculate (4).

$$\begin{cases} \begin{pmatrix} V_1 \\ V_2 \end{pmatrix} = Z_{11} \begin{pmatrix} I_1 \\ I_2 \end{pmatrix} + Z_{12} \begin{pmatrix} I_3 \\ I_4 \end{pmatrix} \\ \begin{pmatrix} V_3 \\ V_4 \end{pmatrix} = Z_{21} \begin{pmatrix} I_1 \\ I_2 \end{pmatrix} + Z_{22} \begin{pmatrix} I_3 \\ I_4 \end{pmatrix} \end{cases} \quad (3)$$

Where:

$$Z_{11} = \begin{bmatrix} z_{11} & z_{12} \\ z_{21} & z_{22} \end{bmatrix} ; Z_{12} = \begin{bmatrix} z_{13} & z_{14} \\ z_{23} & z_{24} \end{bmatrix}$$

$$Z_{21} = \begin{bmatrix} z_{31} & z_{32} \\ z_{41} & z_{42} \end{bmatrix} ; Z_{22} = \begin{bmatrix} z_{33} & z_{34} \\ z_{43} & z_{44} \end{bmatrix}$$

$$T = \begin{bmatrix} Z_{22} \cdot Z_{12}^{-1} & Z_{22} \cdot Z_{12}^{-1} \cdot Z_{11} - Z_{21} \\ Z_{12}^{-1} & Z_{12}^{-1} \cdot Z_{11} \end{bmatrix} \quad (4)$$

(5) is calculated the same way as (4). Using the T matrix the voltages can be calculated in terms of the currents instead calculating the outputs in terms of the inputs.

$$Z = \begin{bmatrix} T_{21}^{-1} \cdot T_{22} & T_{21}^{-1} \\ T_{11} \cdot T_{21}^{-1} \cdot T_{22} - T_{12} & T_{11} \cdot T_{21}^{-1} \end{bmatrix} \quad (5)$$

Where:

$$T_{11} = \begin{bmatrix} t_{11} & t_{12} \\ t_{21} & t_{22} \end{bmatrix} ; T_{12} = \begin{bmatrix} t_{13} & t_{14} \\ t_{23} & t_{24} \end{bmatrix}$$

$$T_{21} = \begin{bmatrix} t_{31} & t_{32} \\ t_{41} & t_{42} \end{bmatrix} ; T_{22} = \begin{bmatrix} t_{33} & t_{34} \\ t_{43} & t_{44} \end{bmatrix}$$

#### D. Load representation

In most cases, the output of a load cannot be electrically measured, because it is not an electric output (e.g. mechanical, acoustic and optical etc). Thus, modeling the load with a pentapolar block is inappropriate. Instead, the load is considered as a tripolar block with only two voltages and two currents as shown in Fig.5. This method can be used for any kind of load.

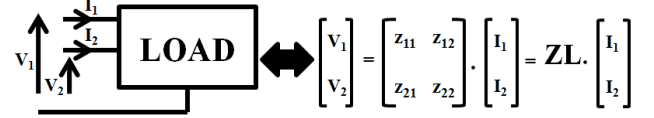


Figure 5. Load representation

The load impedance matrix can be therefore determined using the same methodology as the pentapolar matrix, by determining  $z_{ii}$  and  $z_{ij}$ . (See section I.B)

#### E. Association of a pentapole and a tripole

Once the matrix of the pentapolar block and the tripolar load are defined, (6) can be applied in order to rebuild the passive part of the system in a single tripolar block as shown in Fig.6.

$$\begin{bmatrix} V_1 \\ V_2 \end{bmatrix} = [I_2 + Z_{12} \cdot Z_L^{-1} \cdot T_{11}]^{-1} \times [Z_{11} + Z_{12} \cdot Z_L^{-1} \cdot T_{12}] \begin{bmatrix} I_1 \\ I_2 \end{bmatrix} \quad (6)$$

Where  $Z_L$  is the 2x2 tripolar impedance matrix of the load and  $I_2$  is a 2x2 identity matrix.

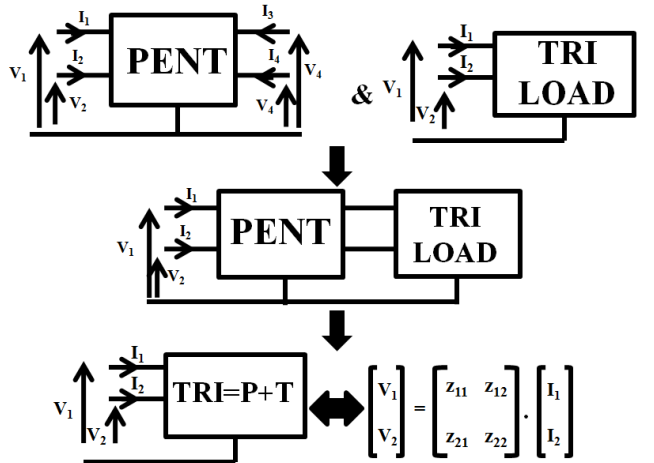


Figure 6. Pentapole and tripole association technique

### III. APPLICATION ON THE OUTPUT CIRCUIT OF A CLASS D AMPLIFIER

The proposed approach is applied to the passive part of a switching audio amplifier composed of an output filter associated with a loudspeaker. Fig.1 shows the block decomposition of the class D amplification system. The used

filter (Fig.7) is the recommended filter in the evaluation kit of the class D amplifier MAXIM 9700B [3].

**A. Filter matrix determination by measurement**

The impedance matrix of the output filter shown in Fig.7 has been determined using two methods: calculation using the measurement of the filter components to obtain the matrix, and measurement on the complete filter. The impedance meter HP4294a shown in Fig.8 is used for impedance measurements. Two impedance results from the impedance matrix  $z_{11}$  in Fig.10.a and  $z_{23}$  in Fig.10.b are presented.

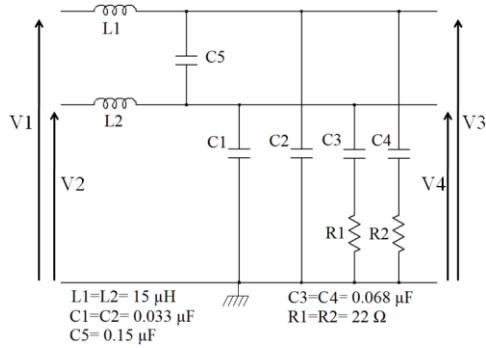


Figure 7. Considered differential filter

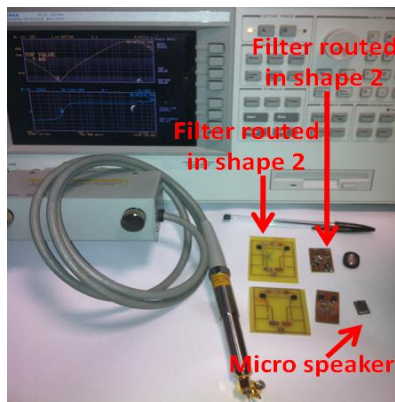


Figure 8. Test bench

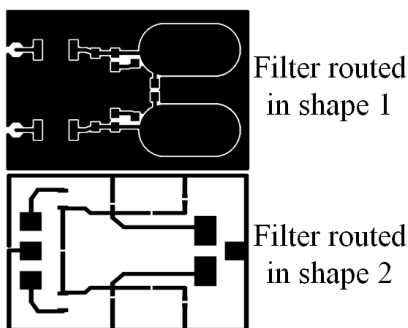
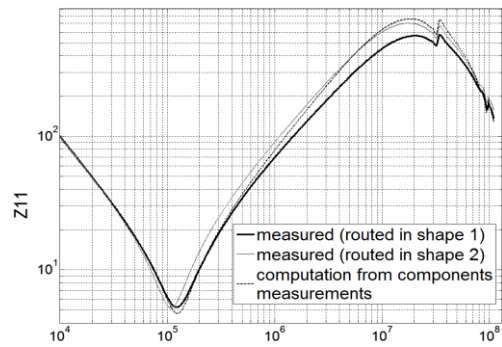
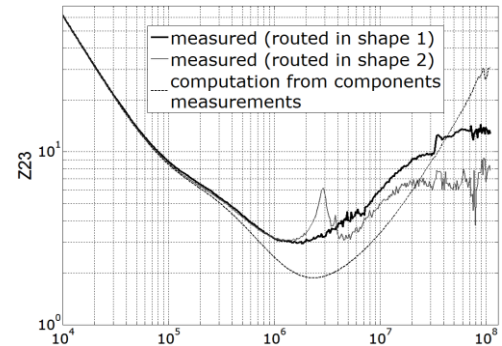


Figure 9. Routings of the filters



(a)



(b)

Figure 10. 2 examples of filter matrix impedances

As can be seen from Fig.10.b, the results show that the cross impedances of the matrix ( $z_{ij}$  with  $i \neq j$ ) calculated using component measurements and calculated using (2) are not similar at high frequencies, and that because of the tracks impedances and the parasitic coupling between the components. In order to verify this hypothesis, two routing shapes for the filter are considered (Fig.9). Results in Fig.10.b show the difference between  $z_{23}$  in the case of a filter routed in shape 1 and a filter routed in shape 2. The differences can be explained by the variation of parasitic elements of tracks and the variation of couplings between components. Therefore, the declared hypothesis is considered verified. This phenomenon has been highlighted in previous work [16-17] but it is difficult to take into account. To limit this phenomenon and to neglect its effects, only “good practices” in routing and component placement are cited as the solution [18-19]. [20] propose an innovative model to take into account coupling between components but it should be noted that this method is in early development.

**B. Loudspeaker matrix determination and variation analysis**

For a precise validation, the stability of the load impedance is explored. The impedance of the speaker is measured with different positions of the vibrating membrane, by applying a positive or negative bias that moves the membrane forward or backward. Fig.11 shows the measured impedances.

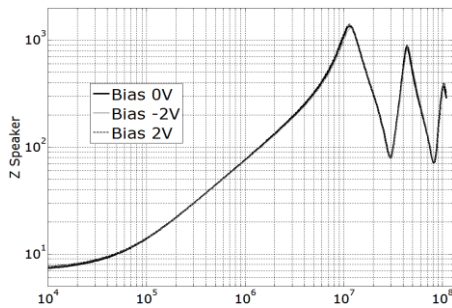


Figure 11. Speaker's impedance at different membrane position

From Fig.11, it clearly appears that the position of the membrane has a low impact on the speaker's impedance, which implies that there is negligible dependence on the conducted EMI prediction. Hence, the speaker load is modeled with a tripolar impedance matrix (see section II-D). It is important to note that the speaker impedance varies also with mechanical parameters variation and temperature drift.

### C. Experimental validation of the matrices association

In order to experimentally validate the association method, (6) is used to associate the pentapolar filter block and tripolar speaker block (Fig.12). The results of the physical association and mathematical association are shown in Fig.13.a and Fig.13.b.

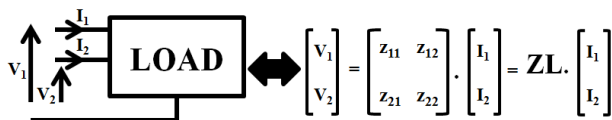


Figure 12. Filter, loudspeaker association

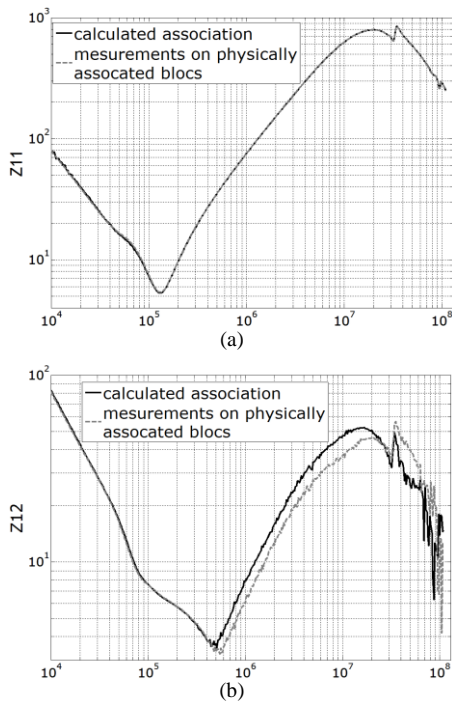


Figure 13. matrix's elements of the associated filter and loudspeaker

As can be clearly seen in Fig.13.a, the two curves (mathematical + physical) superimpose. Although, even if in Fig.13.b the curves are not completely overlapping, they show a sufficient accuracy for the used association method. Note that  $Z_{11}$  and  $Z_{22}$  are quite similar since the system is symmetric. The non-null values of  $Z_{12}$  highlight the mode conversion phenomenon.

## IV. CONCLUSION

The proposed approach models the conducted EMI paths with blocks, and predicts the behavior of a complete system composed of several blocks including their imperfections. Each block can be determined using measurements, calculations or simulations. This approach offers a short simulation time and has the ability to model differential and common mode perturbations as well as mode conversion for single blocks and for a complete passive system. This model will be useful for EMI engineers, as well as system-level designers, for EMC predictions and for normative comparisons. It should be noted that, in this paper, the proposed model is applied to a differential filter connected to a loudspeaker but it could also be applied to any passive system with two active conductors and a ground reference.

In future work this approach will be used for passive block conception such as filters and loads, with the aim of an EMI behavior optimization. Moreover, this approach will be generalized to three-phase and N-phase systems so it can be used to model complex power electronics systems.

## REFERENCES

- [1] Akue Boulingui, S. Dupoux, C. Baffreau, S. Sicard, E. Bouvier, N. Vignon, B. "An innovative methodology for evaluating multi-chip EMC in advanced 3G mobile platforms", Electromagnetic Compatibility 2009. EMC 2009. IEEE International Symposium .
- [2] Vives-Gilbert, Y. Arcambal, C. Louis, A. Eudeline, P. Mazari, B. "Modeling Magnetic Emissions Combining Image Processing and an Optimization Algorithm" Electromagnetic Compatibility, IEEE Transactions. Octobre 2009.
- [3] MAXIM 9700B datasheet <http://www.maxim.com/datasheet/index.mvp/id/4275> [Revised May 6, 2011].
- [4] Siniscalchi, P.P. and R.K. Hester, "A 20 W/Channel Class-D Amplifier With Near-Zero Common-Mode Radiated Emissions" Solid-State Circuits, IEEE Journal. Volume: 44, Issue: 12. Page(s): 3264 – 3271. Decembre 2009.
- [5] Xin Ming, Zao Chen. "An Advanced Spread Spectrum Architecture Using Pseudorandom Modulation to Improve EMI in Class D Amplifier" Power Electronics, IEEE Transactions. August 2010.
- [6] Mei-Ling Yeh Wan-Rone Liou Hsiang-Po Hsieh Yu-Jei Lin. "An Electromagnetic Interference (EMI) Reduced High-Efficiency Switching Power Amplifier" Power Electronics, IEEE Transactions. November 2009.
- [7] Paramesh, J. von Jouanne, A. "Use of sigma-delta modulation to control EMI from switch-mode power supplies" Industrial Electronics, IEEE Transactions. August 2002.
- [8] C.F. Edwards "Efficient switching output stages methods" U.S. Patent 7190225, 13 Mar 2007.
- [9] Jettanassen, C., F. Costa, and C. Vollaïre, "Common-Mode Emissions Measurements and Simulation in Variable-Speed Drive Systems" Power Electronics, IEEE Transactions, 2009. 24(11): p. 2456-2464.
- [10] Jettanassen, C. Costa, F. Vollaïre, C. Revol, B. Morel, F. "Measurements and Simulation of Common Mode Conducted Noise Emissions in

- Adjustable-Speed AC Drive Systems” Electromagnetic Compatibility, 2009 20th International Zurich Symposium on. 2009.
- [11] Costa, F., C. Vollaïre, and R. Meuret, “Modeling of conducted common mode perturbations in variable-speed drive systems” Electromagnetic Compatibility, IEEE Transactions on, 2005. 47(4): p. 1012-1021.
- [12] Regue, J.-R. Ribo, M. Duran, D. Badia, D. Perez, A. “Common and differential mode characterization of EMI power-line filters from S-parameters measurements” Electromagnetic Compatibility, 2004. EMC 2004. 2004 International Symposium on. 2004.
- [13] Hagmann, J.H. and S. Dickmann. “Determination of mode conversion on differential lines” Electromagnetic Compatibility - EMC Europe, 2008 International Symposium 2008.
- [14] Aime, J. Clavel, E. Roudet, J. Baudesson, P. “Determination of the layout influence on the effectiveness of a three-phase common mode filter by using equivalent circuits and PSpice” Industrial Electronics, 2008. ISIE 2008. IEEE International Symposium 2008.
- [15] Chen, S. Nehl, T.W. Lai, J.-S. Huang, X. Pepa, E. De Doncker, R. Voss, I. “Towards EMI prediction of a PM motor drive for automotive applications” Applied Power Electronics Conference and Exposition, 2003. APEC '03. Eighteenth Annual IEEE. 2003.
- [16] Shuo Wang Lee, Fred.C. Odendaal, W.G. van Wyk, J.D. “Improvement of EMI filter performance with parasitic coupling cancellation” Power Electronics, IEEE Transactions on, 2005. 20(5): p. 1221-1228.
- [17] Shuo Wang Rengang Chen Van Wyk, J.D. Lee, Fred.C. Odendaal, W.G. “Developing parasitic cancellation technologies to improve EMI filter performance for switching mode power supplies” Electromagnetic Compatibility, IEEE Transactions on, 2005. 47(4): p. 921-929.
- [18] Shuo, W. and F.C. Lee, “Common-Mode Noise Reduction for Power Factor Correction Circuit With Parasitic Capacitance Cancellation” Electromagnetic Compatibility, IEEE Transactions on, 2007. 49(3): p. 537-542.
- [19] Shuo, W., F.C. Lee, and J.D. van Wyk, “A Study of Integration of Parasitic Cancellation Techniques for EMI Filter Design With Discrete Components” Power Electronics, IEEE Transactions on, 2008. 23(6): p. 3094-3102.
- [20] Zangui, S. Vincent, B. Berger, K. Perrussel, R. Clavel, E. Vollaïre, C. Chadebec, O. “Near-field coupling between EMC filter components” Electromagnetic Field Computation (CEFC), 2010 14th Biennial IEEE Conference 2010.